



## Nutritional properties and osteogenic activity of simulated digestion components and peptides from *Larimichthys crocea*

Zhe Xu<sup>a,b</sup>, Shiyang Han<sup>a</sup>, Hui Chen<sup>c</sup>, Lingyu Han<sup>a</sup>, Xiufang Dong<sup>e</sup>, Maolin Tu<sup>f</sup>, Zhijian Tan<sup>b,\*</sup>, Ming Du<sup>d,\*</sup>, Tingting Li<sup>a,\*</sup>

<sup>a</sup> College of Life Sciences, Key Laboratory of Biotechnology and Bioresources Utilization, Dalian Minzu University, Ministry of Education, Dalian 116029, China

<sup>b</sup> Institute of Bast Fiber Crops & Center of Southern Economic Crops, Chinese Academy of Agricultural Sciences, Changsha 410205, China

<sup>c</sup> Key Laboratory of Marine Fishery Resources Exploitation & Utilization of Zhejiang Province, Zhejiang University of Technology, Hangzhou 310014, China

<sup>d</sup> School of Food Science and Technology, National Engineering Research Center of Seafood, Collaborative Innovation Center of Seafood Deep Processing, Dalian Polytechnic University, Dalian 116034, China

<sup>e</sup> College of Marine Science and Biological Engineering, Qingdao University of Science and Technology, Qingdao 266042, China

<sup>f</sup> Key Laboratory of Animal Protein Food Deep Processing Technology of Zhejiang Province, College of Food and Pharmaceutical Sciences, Ningbo University, Ningbo 315832, China

### ARTICLE INFO

#### Keywords:

*Larimichthys crocea*

Digestion

Protein

Osteoblasts

Function

### ABSTRACT

Fish provides a range of health benefits due to its nutritional and bioactive components. However, the bioactive peptides derived from *Larimichthys crocea* proteins were not fully investigated, especially the beneficial effects related to bone growth *in vitro*. In this study, the water extract protein was subjected to the simulated *in vitro* digestion process, and the osteogenic effect of enzymatic hydrolysate at different digestion stages was evaluated by the proliferation of osteoblast. The protein hydrolyzates of group pepsin treatment for 1 h and pepsin treatment for 2 h showed higher osteogenic activity *in vitro*. Two peptides including IERGDVVVQDPSD from pepsin treatment for 1 h and RGDLGIEIPTEK from pepsin treatment for 2 h were identified, which revealed eminent effects in terms of promoting osteoblast proliferation and enhancing ALP activity. Moreover, the available nutrients in the proteins were determined by the molecular weight distribution and free amino acid composition. Those peptides also showed stronger interaction with RGD than integrins. Therefore, the peptides from *Larimichthys crocea* can be used as an effective ingredient for promoting bone growth in the future.

### 1. Introduction

The dynamic balance of bone resorption and bone formation in human body has been viewed as consequential to maintain healthy activity of bones. Osteoclasts break down and absorb the existing bone, while osteoblasts direct the synthesis of new matrix to fill the bone vacuum (Fan et al., 2017). In recent decades, osteoporosis has become a common disease, due to the endocrine disorders, aging and other factors. Osteoporosis can be divided into primary and secondary osteoporosis, and primary osteoporosis can be further divided into postmenopausal and age-related osteoporosis. Postmenopausal bone loss is exacerbated by the lack of estrogen in human body. Calcitriol is deficient as people's age, resulting in the decline of calcium absorption. Secondary osteoporosis is mainly caused by a number of diseases, treatments, medications, lifestyles, etc. At present, there are about 200 million patients suffering from osteoporosis. As the aging population in

China increased, the prevalence of osteoporosis was also rising. Hitherto the number of patients with osteoporosis in China is up to 90 million. Therefore, the prevention and treatment of osteoporosis is becoming a public health problem.

Osteoblasts are vital cells in bone reconstruction which can secrete many active substances to promote bone formation. Some bioactive substances can promote osteoblasts differentiation, such as bone morphogenetic protein (Hughes, Turner, Belibasakis, & Martuscelli, 2006), which is the main factor of bone formation *in vivo*, that promotes the expression of alkaline phosphatase (ALP) (Canalis, Economides, & Gazzero, 2003; Kim, Kim, Kim, Seong, & Kim, 2018). ALP is an exoenzyme located on osteoblasts and a specific indicator of osteoblast differentiation (Georgy et al., 2012; Kim et al., 2018). Tartrate-resistant acid phosphatase (TRAP) is a specific and highly sensitive bone resorption indicator (Georgy et al., 2012; Haider et

\* Corresponding authors.

E-mail addresses: [tanzhijian@caas.cn](mailto:tanzhijian@caas.cn) (Z. Tan), [duming@dlpu.edu.cn](mailto:duming@dlpu.edu.cn) (M. Du), [jwltt@dlnu.edu.cn](mailto:jwltt@dlnu.edu.cn) (T. Li).

<https://doi.org/10.1016/j.foodres.2022.112238>

Received 15 July 2022; Received in revised form 16 November 2022; Accepted 23 November 2022

0963-9969/© 20XX

al., 2015). Previous studies have shown that proteins or peptides could promote osteoblast proliferation and differentiation or inhibit osteoclast differentiation to increase bone formation and inhibit bone resorption (Bharadwaj, Naidu, Betageri, Prasadarao, & Naidu, 2009; Cornish et al., 2004; Li, Zhu, & Hu, 2015). The protein such as lactoferrin can promote the growth of osteoblasts (Naot et al., 2011; Wang et al., 2013), and reduce the differentiation of osteoclasts *in vitro* (Blais, Malet, Mikogami, Martin-Rouas, & Tomé, 2009; Lorget et al., 2002).

Studies have shown that most seafood is rich in proteins and contains all the essential amino acids. High-protein seafood can be digested by the gastrointestinal tract into small molecular peptides (Chen et al., 2019; Jeong et al., 2018; Xu et al., 2019b). Small molecule peptides often have good biological activity (Chen et al., 2019; Lin, Zhang, Han, & Cheng, 2017). In the study by Hyung et al., large yellow croaker (*Larimichthys crocea*) showed high nutritional value and certain medicinal value. It has good anti-inflammatory effect in human body (Hyung, Ahn, & Je, 2018).

However, studies on the activity of large yellow croaker protein in promoting bone health are still limited. This study focused on the water-soluble protein extracted from large yellow croaker (WPL), and the bioactive peptides released after *in vitro* gastrointestinal digestion. The effect of those peptides on proliferation and differentiation of osteoblasts was evaluated by the determination of composition and molecular weight distribution. Amino acid analysis was also performed to characterize the large yellow croaker hydrolysate. This study may improve the application of WPL in osteoporosis treatment and provide new insights into skeletal disorders.

## 2. Materials and methods

### 2.1. Materials

*Larimichthys crocea* were purchased from the local seafood market in Dalian, Liaoning Province, China. Penicillin-streptomycin,  $\alpha$ -MEM medium, and fetal bovine serum were sourced from Gibco, USA. MC3T3-E1 pre-osteoblasts cells were obtained from Shanghai Academy of Sciences, China. Formic acid was mass spectrometry grade. Alkaline phosphatase (ALP) test kit was from Beyotime, China. Acetonitrile (ACN) was liquid chromatography grade obtained from Merck, Germany.

### 2.2. *Larimichthys crocea* protein *in vitro* digestion

*Larimichthys crocea* were repeatedly washed with water to remove impurities and salts. Then, the large yellow croaker was pretreated to remove the head, skin, bone, and viscera. The pretreated samples were mixed with water at a mixing ratio of 1:3 (w/w). A JYL-Y28 homogenizer was used to homogenize the mixture for 4 h at 4 °C and 60 rpm. Thereafter, the protein solution was centrifuged at 10,000 g for 10 min in a Hitachi centrifuge (CR22N), and the supernatant was removed for freeze-drying.

The protein solution of large yellow croaker hydrolyzed under different conditions was divided into 5 groups. The first group was hydrolyzed with pepsin for 1 h, denoted as P1; the second group was hydrolyzed under the condition of pepsin for 2 h, denoted as P2; The third group was hydrolyzed under pepsin condition for 2 h, then hydrolyzed with trypsin for 1 h, denoted as P2T1; the fourth group was hydrolyzed under pepsin condition for 2 h, then hydrolyzed with trypsin for 2 h, denoted as P2T2; and the fifth group was hydrolyzed with pepsin for 2 h, and then hydrolyzed under trypsin condition for 3 h, denoted as P2T3. The optimum pH of the solution was regulated by using HCl or NaOH, and the optimum temperature (37 °C) was ad-

justed with water bath heating. The optimum pH for pepsin and trypsin were 2.0 and 8.0, respectively. Substrate protein was digested with 5000 U/g protein each enzyme. Subsequently, the enzymolysis solution was stirred at a speed of 60 rpm during digestion, and the enzymes were finally inactivated by boiling water.

### 2.3. SDS-PAGE

In brief, WPL and its hydrolysates were separated by polyacrylamide gel electrophoresis (SDS-PAGE) (Laemmli, 1970), which consisted of 3 % concentrated gel and 15 % isolated gel. The same concentration of large yellow croaker protein solution and its hydrolysate were dissolved in loading buffer solution consisting of 0.02 %  $\beta$ -mercaptoethanol, 0.01 % bromophenol blue (BPB), 4 % SDS, 0.125 M Tris-HCl, and 20 % glycerol composition. The gels were then stained with Coomassie Brilliant Blue G-250 and finally eluted with eluent, and scanned overnight by using a Bio-imaging systems instrument.

### 2.4. Determination of molecular weight of peptides

The size exclusion chromatography was improved according to the relevant experimental methods (Song et al., 2018). The relative molecular weight of polypeptides was determined by Xultimate *sEC*-120 (7.8 × 300 mm) column. The mobile phase consisted of 45 % acetonitrile with 0.1 % trifluoroacetic acid aqueous solution, with 10  $\mu$ L of sample loading solution; the column temperature was 30 °C; and the flow rate was 0.5 mL/min. Lysine with molecular weight of 146.20 Da, Gly-Gly-Tyr-Arg of 451.48 Da, and Glu-lys-val-Asn-glu-leu-ser-Lys of 1072.05 Da, Aprotinin of 6511.44 Da and Cytochrome C of 12384.00 Da were determined as standard. The linear relationship between retention time and average molecular weight (Lg MW) was determined by standard curve. There are three independent replicates performed.

### 2.5. Amino acids analysis

The automatic amino acid analyzer used in the experiment was LA8080 produced by Hitachi, Japan, equipped with a cation exchange chromatographic column. For the analysis of free amino acids of large yellow croaker protein, the temperature was set at 57 °C. All samples were deproteinized in the experiment. Firstly, insoluble matter was removed by a centrifuge (CR22N, Hitachi, Japan) for 10 min at 10,000 g. Acetone was then added to the solution and centrifuged at 10,000 g for 10 min. Finally, 0.02 M HCl was added to the solution, and the samples were drawn with a syringe and injected onto a 0.45  $\mu$ m filter membrane for filtration.

### 2.6. Instrumentation and chromatographic condition

The analysis conditions of UPLC Q Exactive™ HF-X (Thermo, USA) are consistent with those published (Yang & Xu, 2021). Maxquant (V1.6.15.0) was used to analyze the secondary mass spectrometry data. The database was *Larimichthys crocea*\_215358\_PR\_20210628. In order to eliminate the influence of contamination on the identification results, the fastA (23,960 sequences) file was loaded, and the anti-database was added to calculate the false positive rate (FDR) caused by random matching. Meanwhile, a common contamination database was also added to the database. The mass tolerance of the secondary fragment ion was set to 20 ppm; the mass tolerance of the precursor ion was set to 20 ppm and 4.5 ppm, respectively; and the maximum number of peptide modifications was set to 5. The minimum peptide length was set to 7 amino acid residues. The number of missing cleavage sites was set to 2. The alkylation of cysteine with methyl carbamate was set as

fixed modification. The oxidation of methionine, acetylation of protein *n*-terminal, and deamidation were set as variable modification. FDR was set at 1 % for PSM and protein identification.

In order to obtain high-quality analysis results, the search database analysis results were further filtered. The FDR was set to 1 % for the accuracy of identification at the three levels of spectrum, peptide, and protein. Table S1 (Supplementary information) shows the total number of peptides and proteins identified after data filtering in the database search results.

### 2.7. MTT assay

MTT colorimetry assay was used to detect the effect of samples on the proliferation of MC3T3-E1 cells, which reflected the number of viable cells (Chen et al., 2014). Cells were grown in 100  $\mu$ L of  $\alpha$ -MEM and seeded at  $5 \times 10^4$  cells/mL in 96-well culture plates (Kim, Kim, Jung, Hong, & Lee, 2014; Liu et al., 2019). The plates were transferred to 5 % CO<sub>2</sub> atmosphere and incubated for 24 h, then MC3T3-E1 cells were treated with medium at 37 °C, hydrolysed for 24, 48 and 72 h. MTT solution (10  $\mu$ L) was added and incubated with cells for another 4 h. Thereafter, 150  $\mu$ L of dimethyl sulfoxide was added to each well. A microplate reader (Eon, BioTek, USA) was used to measure the absorbance at OD570 nm wavelength.

### 2.8. ALP activity assay

The sample was incubated with MC3T3-E1 cells for three days, and cell alkaline phosphatase activity was then measured by using an alkaline phosphatase detection kit (Beyotime Biotechnology, Shanghai, China).

### 2.9. Molecular docking

Molecular docking was performed with Discovery Studio 2017 software. Potential peptides with osteogenic activity were docked with integrins (PDB: 3VI4, 1L5G). The RGD peptide ligands and co-crystal structures of integrins were obtained from Protein Data Bank (PDB: 3VI4, 1L5G). The crystal structure of integrin (PDB: 3VI4, 1L5G) (Takagi, Strokovich, Springer, & Walz, 2003; Xiong et al., 2002) was used as the template molecule target peptide, and the optimal peptide was screened by scoring. CDocker is the main docking algorithm in the Discovery Studio software and it was used as the RGD-Peptide model. The receptor was removed from the overall crystal structure of the RGD ligand and water, and the interaction site of RGD with the biologically active peptide was the starting position of RGD docking at 3VI4 or 1L5G. The energy minimization and the structure of the target peptide were calculated based on the amino acid sequence of the target peptide, followed by molecular docking. During the molecular docking process, the type of interaction between the receptor and the ligand was determined (Zhang et al., 2016).

### 2.10. Preparation of osteogenic peptides

The polypeptides with the highest osteogenic activity were screened in the hydrolysis products. The peptide was chemically synthesized by ChinaPeptides Co., Ltd. in Shanghai, China, and were further characterized by high performance liquid chromatography (HPLC)/mass spectrometry. The HPLC was LC6000N from Beijing Chuangxin Tongheng Chromatographic Technology Co., Ltd, China, and the ESI-MS was ZQ2000 from Waters, USA. The HPLC method conditions were: Kromasil 100-5C18, Thermo Fisher HPLC system, with the flow rate of 1.0 mL/min, and the concentration of synthetic peptide was 1.0 mg/

mL. RGDGIEIPEK with elution buffer A to 0.1 % TFA in acetonitrile, then RGD with buffer A with 0.1 % TFA in water. Elution buffer A was eluted to 17 %, then eluted to 42 % after 20 min, until the gradient elution reached 100 % in another 5 min. IERGDVVVQDSPSD buffer A and buffer B were 0.1 % TFA in acetonitrile, and 0.1 % TFA in water, respectively. The gradient parameter of buffer A was: 40 %, 20 min, 100 % 5 min. ESI source parameters were set as follows: capillary,  $\pm$  (2500–3000); dissolution temperature (TEM), 450 °C; anti-solvent (L/HR): 800; cone (V): 30–50.

### 2.11. Statistical analysis

All data are presented as mean  $\pm$  standard deviation. Relevant tests shall be repeated at least three times independently. The level of significance ( $p < 0.05$ ) was determined with Duncan's (D) post hoc test. OriginPro 2016 was used for data processing. SPSS 19.0 software was used to conduct one-way analysis of variance for the experimental data.

## 3. Results and discussion

### 3.1. Properties of WPL

The SDS-PAGE of simulated digestion of large yellow croaker protein at different time intervals (*P*<sub>1</sub>, *P*<sub>2</sub>, *P*<sub>2T1</sub>, *P*<sub>2T2</sub>, *P*<sub>2T3</sub>) are presented in Fig. 1A. Electrophoretic images showed that the WPL bands were different from the simulated digestion bands. Notably, the protein bands digested by pepsin showed the most significant difference. WPL was digested by pepsin into components with a molecular weight of 11–245 kDa, and the protein or polypeptide with a molecular weight of 5–11 kDa was released during the digestive gastric phase, which disappeared in intestinal digestion. During the trypsin treatment stage (1–3 h), the water-soluble protein of large yellow croaker was hydrolyzed into free amino acids or small peptides, which was slightly different with the simulation effect related to blue mussel protein (Xu, Zhao, et al., 2019). As a result, the water-soluble protein of large yellow croaker was more likely to be degraded into small molecular peptides during the simulated digestion process, which implied that the water-soluble protein of large yellow croaker was easier to be digested.

### 3.2. Molecular weight distribution of protein hydrolysates

In the different stages of simulated digestion, pepsin and trypsin had different molecular weight distribution. As shown in Fig. 1B, after the simulated mussel protein digestion process, the complete protein was gradually broken down into amino acids or smaller peptides with the increase of hydrolysis time. Proteins greater than 3000 Da were also reduced, and the components (< 3000 Da) in *P*<sub>2T3</sub> group reached 90.2 %. According to some previous studies, peptides with molecular weight < 3000 Da showed good bioactivity because they are more easily absorbed and utilized (Fernández-Musoles, Manzanares, Burguete, Alborch, & Salom, 2013; Lin, Zhang, Han, & Cheng, 2017; Ruiz-Giménez et al., 2012). As expected, the components in *P*<sub>1</sub> group were mainly distributed in 500–3000 Da, which was as high as 29.3 % (Fig. 1C). Therefore, the component in *P*<sub>1</sub> group may have the best osteogenic activity.

### 3.3. Amino acid composition

Free amino acids or short-chain bioactive peptides produced by protein hydrolysis, as well as natural bioactive peptides are confirmed to have high nutritional value in human body (Tak et al., 2021). Table 1 shows the release of free amino acids in the

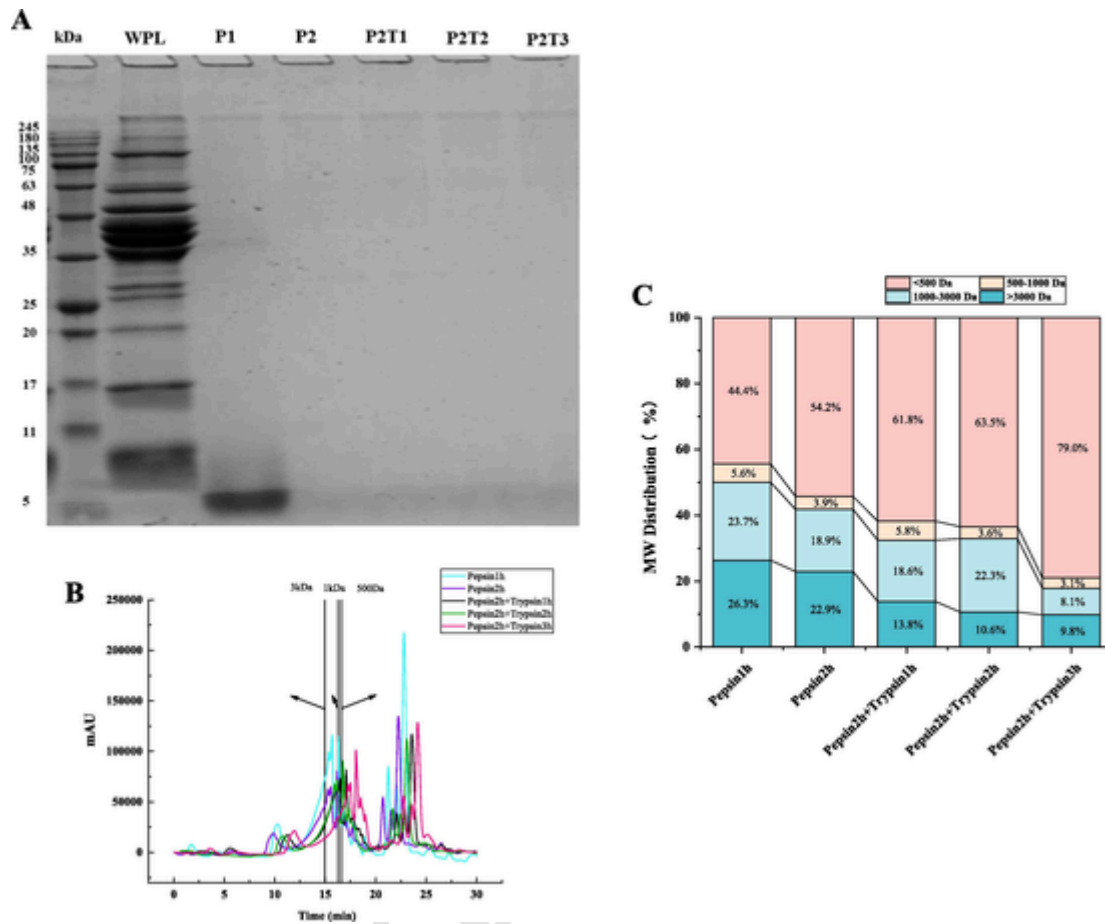


**Fig. 1.** (A) The SDS-PAGE of WPL subjected to *in vitro* simulated gastrointestinal digestion. There are 10  $\mu$ g samples were loaded in each lane. WPL, water-soluble protein from *Larimichthys crocea*; (B-C) In the simulated digestion stage, the molecular weight distribution of components in each stage. P1, pepsin 1 h; P2, pepsin 2 h; P2T1, pepsin 2 h + trypsin 1 h; P2T2, pepsin 2 h + trypsin 2 h; P2T3, pepsin 2 h + trypsin 3 h.

process of simulating WPL *in vitro* gastrointestinal digestion. The hydrolysate was rich in threonine, lysine, leucine, phenylalanine, leucine, and alanine acid, aspartic acid, glutamic acid, and glycine. Compared with the large yellow croaker protein hydrolysate of the control group, the hydrolyzed solution after 2 h of pepsin hydrolysis and 3 h of trypsin hydrolysis showed a significant increase of amino acid contents (Ghassem et al., 2014; Je, Park, Hwang, & Ahn, 2015). As previously described, Arg-Gly-ASP (RGD) peptide could effectively promote the proliferation of osteoblasts (Kang et al., 2018; Tsai, Chen, Wei, Tan, & Lai, 2010). In Table 1, with the prolongation of digestion time, the contents of Arg, Asp and Gly increased slightly, however no significant difference was observed. Therefore, there are more peptides containing RGD. This result was consistent with that shown in Fig. 2.

### 3.4. *In vitro* hydrolysate products identified by UPLC-Q Exactive<sup>TM</sup>HF-X

In recent years, researches have focused on the biologically active polypeptide (Mada et al., 2017; Pandey, Kapila, Kapila, Trivedi, & Karvande, 2018; Xu et al., 2020; Xu et al., 2019b), especially polypeptides with anti-osteoporosis effect (Mada et al., 2017; Xu et al., 2019a). Table S1 (Supplementary information) lists the result of identification of peptides from *in vitro* hydrolysates by UPLC-Q Exactive<sup>TM</sup> HF-X mass spectrometer. After analysis and identification, a total of 4907, 2601, 796, 907, and 877 peptides were identified from five groups, respectively. It can be concluded that the polypeptide fragments obtained by

different enzymes at different digestion stages were different. According to the relevant studies, RGDLEIPIPTK and VARGDLGIEIPTK peptides in Table S1 (Supplementary information) showed better bone bioactivity, indicating the best osteogenic effect of peptides in group P1 and P2 (Xu et al., 2019a). The peptides RGD (Yang et al., 2005), TDLQERGDNDISPFSGDGQPFKD (Nagel et al., 2004), LVQPRG DTNGPGPWQGGRRKFRQRPRLSHKGPMPF (Tang et al., 2007), AGYKPDEGKRGDACEGDSGGPFV (Li, Ryaby, Carney, & Wang, 2005), and YRGDVVPK (Chen et al., 2019) had the same amino acid sequence which has been reported to promote bone formation in bone marrow stromal cells (Mada et al., 2017).

### 3.5. Osteogenic activity of hydrolysates in pre-osteoblasts

WPL and five groups of protein hydrolysate were added into the medium of pre-osteoblasts for 1, 10, and 100  $\mu$ g/mL. All the samples were then cultured for 24 h, 48 h, and 72 h, respectively ( $p < 0.05$ ) (Fig. 2). Compared with the control group (without protein or polypeptide), the pre-osteoblasts increased significantly after the incubation with 100  $\mu$ g/mL WPL, P1, P2, P2T1, P2T2, P2T3 concentration, respectively. With regards to the ratio of MC3T3-E1-preosteoblast proliferation, the WPL, P1, P2, P2T1, P2T2, and P2T3 group in the presence of 100  $\mu$ g/mL showed an increase of  $30.45 \pm 3.13$  %,  $37.60 \pm 7.97$  %,  $32.47 \pm 14.15$  %,  $29.26 \pm 9.34$  %,  $30.24 \pm 2.69$  %, and  $26.58 \pm 4.95$  % after 72 h treatment. Moreover, the ALP activity of WPL, P1, P2, P2T1, P2T2, and P2T3 group in the presence

Table 1

Effect of the release of free amino acids (mg/g) during *in vitro* simulated gastrointestinal digestion of WPL (Mean  $\pm$  SD)\*.

	WPL	Pepsin 1 h	Pepsin 2 h	Pepsin 2 h + Trypsin 1 h	Pepsin 2 h + Trypsin 2 h	Pepsin 2 h + Trypsin 3 h
Essential amino acid						
Threonine (Thr)	1.408 $\pm$ 0.072 <sup>a</sup>	12.102 $\pm$ 0.119 <sup>b</sup>	18.317 $\pm$ 0.311 <sup>b</sup>	20.518 $\pm$ 0.194 <sup>b</sup>	22.513 $\pm$ 0.078 <sup>b</sup>	23.761 $\pm$ 0.075 <sup>b</sup>
Cysteine (Cys)	0.259 $\pm$ 0.047 <sup>a</sup>	0.555 $\pm$ 0.044 <sup>b</sup>	0.705 $\pm$ 0.051 <sup>b</sup>	0.815 $\pm$ 0.048 <sup>b</sup>	0.884 $\pm$ 0.041 <sup>b</sup>	0.915 $\pm$ 0.052 <sup>b</sup>
Lysine (Lys)	4.572 $\pm$ 0.055 <sup>b</sup>	7.883 $\pm$ 0.060 <sup>a</sup>	8.417 $\pm$ 0.262 <sup>a</sup>	9.081 $\pm$ 0.075 <sup>b</sup>	9.994 $\pm$ 0.079 <sup>c</sup>	9.895 $\pm$ 0.061 <sup>bc</sup>
Methionine (Met)	0.378 $\pm$ 0.058 <sup>b</sup>	0.558 $\pm$ 0.057 <sup>b</sup>	0.915 $\pm$ 0.064 <sup>b</sup>	1.030 $\pm$ 0.062 <sup>a</sup>	1.118 $\pm$ 0.064 <sup>a</sup>	1.148 $\pm$ 0.063 <sup>a</sup>
Phenylalanine (Phe)	1.918 $\pm$ 0.066 <sup>a</sup>	8.407 $\pm$ 0.108 <sup>a</sup>	9.471 $\pm$ 0.202 <sup>a</sup>	10.523 $\pm$ 0.068	11.508 $\pm$ 0.061 <sup>ab</sup>	11.876 $\pm$ 0.066 <sup>b</sup>
Isoleucine (Ile)	0.167 $\pm$ 0.051 <sup>a</sup>	0.197 $\pm$ 0.052 <sup>a</sup>	0.199 $\pm$ 0.055 <sup>a</sup>	0.212 $\pm$ 0.051 <sup>a</sup>	0.256 $\pm$ 0.047 <sup>a</sup>	0.241 $\pm$ 0.052 <sup>a</sup>
Leucine (Leu)	0.517 $\pm$ 0.050 <sup>a</sup>	0.968 $\pm$ 0.049 <sup>b</sup>	1.350 $\pm$ 0.063 <sup>c</sup>	1.510 $\pm$ 0.055 <sup>c</sup>	1.725 $\pm$ 0.051 <sup>c</sup>	1.941 $\pm$ 0.071 <sup>c</sup>
Histidine (His)	1.686 $\pm$ 0.059 <sup>a</sup>	3.940 $\pm$ 0.060 <sup>a</sup>	4.581 $\pm$ 0.129 <sup>a</sup>	5.030 $\pm$ 0.063 <sup>ab</sup>	5.593 $\pm$ 0.075 <sup>b</sup>	5.787 $\pm$ 0.084 <sup>b</sup>
Tyrosine (Tyr)	0.293 $\pm$ 0.047 <sup>a</sup>	1.065 $\pm$ 0.058 <sup>b</sup>	2.847 $\pm$ 0.064 <sup>c</sup>	3.800 $\pm$ 0.348 <sup>d</sup>	4.301 $\pm$ 0.730 <sup>de</sup>	4.786 $\pm$ 0.716 <sup>e</sup>
Valine (Val)	1.286 $\pm$ 0.047 <sup>a</sup>	2.058 $\pm$ 0.049 <sup>bc</sup>	2.507 $\pm$ 0.061 <sup>c</sup>	2.676 $\pm$ 0.053 <sup>b</sup>	2.828 $\pm$ 0.040 <sup>bc</sup>	2.893 $\pm$ 0.072 <sup>bc</sup>
Non-essential amino acid						
Serine (Ser)	1.952 $\pm$ 0.039 <sup>a</sup>	2.617 $\pm$ 0.040 <sup>b</sup>	2.472 $\pm$ 0.108 <sup>b</sup>	2.568 $\pm$ 0.044 <sup>b</sup>	2.812 $\pm$ 0.100 <sup>b</sup>	2.764 $\pm$ 0.044 <sup>b</sup>
Arginine (Arg)	–	–	–	0.550 $\pm$ 0.049 <sup>c</sup>	0.706 $\pm$ 0.075 <sup>d</sup>	0.725 $\pm$ 0.086 <sup>cd</sup>
Aspartic acid (Asp)	2.101 $\pm$ 0.050 <sup>a</sup>	2.418 $\pm$ 0.051 <sup>b</sup>	2.411 $\pm$ 0.110 <sup>b</sup>	2.506 $\pm$ 0.054 <sup>b</sup>	2.676 $\pm$ 0.045 <sup>b</sup>	2.749 $\pm$ 0.064 <sup>b</sup>
Glycine (Gly)	1.799 $\pm$ 0.030 <sup>a</sup>	2.096 $\pm$ 0.027 <sup>b</sup>	2.096 $\pm$ 0.091 <sup>b</sup>	2.165 $\pm$ 0.040 <sup>b</sup>	2.258 $\pm$ 0.026 <sup>b</sup>	2.336 $\pm$ 0.032 <sup>b</sup>
Glutamic acid (Glu)	3.223 $\pm$ 0.055 <sup>a</sup>	3.803 $\pm$ 0.058 <sup>b</sup>	3.925 $\pm$ 0.146 <sup>b</sup>	4.196 $\pm$ 0.061 <sup>b</sup>	4.640 $\pm$ 0.057 <sup>b</sup>	4.861 $\pm$ 0.063 <sup>b</sup>
Alanine (Ala)	3.353 $\pm$ 0.030 <sup>a</sup>	4.189 $\pm$ 0.038 <sup>b</sup>	4.351 $\pm$ 0.134 <sup>b</sup>	4.547 $\pm$ 0.041 <sup>b</sup>	4.944 $\pm$ 0.035 <sup>b</sup>	5.016 $\pm$ 0.054 <sup>b</sup>
Proline (Pro)	–	–	–	–	–	–
Total	26.834	54.435	64.386	70.710	77.487	79.965
Major taste component						
Bitter*	5.952	16.127	19.022	20.980	23.027	23.887
Umami*	5.324	6.221	6.337	6.702	7.316	7.610
Sweet*	9.319	11.547	11.587	12.065	13.047	13.173

Annotation: Different lowercase in the same line represent the significant difference at  $p < 0.05$ . “–” indicates that the content is below the detection line or does not exist. \* Bitter: calculated from the sum of leucine, valine, histidine, isoleucine, phenylalanine and methionine; Umami: calculated from the sum of glutamic acid and aspartic acid; Sweet: calculated from the sum of threonine, serine, alanine and glycine.

of 100  $\mu\text{g}/\text{mL}$  were  $1.33 \pm 0.02$  mU,  $1.39 \pm 0.02$  mU,  $1.36 \pm 0.03$  mU,  $1.27 \pm 0.02$  mU,  $1.38 \pm 0.02$  mU, and  $1.32 \pm 0.03$  mU, respectively, which were higher than the control group ( $1.19 \pm 0.04$  mU). ALP activity is one of the biomarkers in response to pre-osteoblasts differentiation and mineralization (Yang et al., 2021). All the above samples can affect the increase of ALP activity, indicating that it can further promote pre-osteoblasts differentiation.

### 3.6. Interaction of peptides with integrins

Bioactive peptides are a general term for different peptides from dipeptides to complex linear and cyclic structures composed of 20 natural amino acids in different compositions and arrangements (Shi et al., 2018). These peptides can bind to specific receptors, regulate the metabolism and various physiological functions of the human body, and can also induce osteoblast differentiation *in vitro* (Oh et al., 2017). In addition, studies have shown that integrin  $\alpha\text{v}\beta 3$  could activate Shc pathway and FAK pathway. Most importantly, the integrin-RGD complex can induce accelerated cell cycle progression (Ashe, 2016; Danen & Yamada, 2001). In the group P2, the active site of integrin on RGD was set as the binding site of the polypeptide, so as to screen the polypeptide which could stimulate or inhibit the proliferation of osteoblasts. Integrin  $\beta 1$  plays a key role in the promotion of osteoblast proliferation by RYVFFKQYWE peptide (Cornish et al., 2004; Lemieux, Horowitz, & Kacena, 2010; Mai et al., 2013; Min, Kang, Jung, Jang, & Min, 2018; Zhou, Zu, Zhuang, & Yang, 2015). Integrin  $\alpha 5\beta 1$  can promote the proliferation and differentiation of osteoblasts, as well as promote the adhesion of osteoblasts. Peptides can interfere with integrin  $\alpha\text{v}\beta 3$ , which is an important protein on the osteoclast membrane that affects the movement and bone resorption capacity of osteoclasts, and inhibit the proliferation of osteoclasts (Park et al., 2016; Zhou et al., 2015). Therefore, RGD may play a key

role in the role of extracellular matrix and integrins. Polypeptides with potential RGD activity are indicators of promoting osteoblast proliferation and inhibiting osteoclast proliferation. The CDOCKER docking algorithm of Discovery Studio 2017 software was used in the experiment. According to the molecular dynamics schematic diagram and the receptor-ligand interaction scoring function under the CHARMM force field, the interaction between RGD and bioactive peptides can be estimated successfully. Meanwhile, the gap of RGD was chosen as the binding site. (Rao, Head, Kulkarni, & LaLonde, 2007). The peptides identified by HPLC-MS were then molecularly docked with RGD. The selected CDOCKER parameter is the most suitable parameter when the interaction between acceptor and donor is the highest one (Wu, Robertson, Brooks, & Vieth, 2003). The energy value was obtained by using the CDOCKER algorithm presented in Table 2. As for the interaction amino acid of IERGDVVVQDSPSD with integrin (PDB: 1L5G, 3VI4), the amino acids that RGDN interacted with integrin  $\alpha 5\beta 1$  (PDB: 3VI4) were PHE187, SER134, ASN224, ASP259, GLU229, LYS182, SER132, LEU225, ASP226, GLU320, CYS187, and SER227, respectively. As for IERGDVVVQDSPSD interacted with integrin  $\alpha 5\beta 1$  (PDB: 3VI4), the related amino acids were PRO127, TRP157, PRO180, ALA181, LYS182, ARG184, PHE187, THR188, LEU225, ILE225, SER227, ASP227, LEU257, ALA260, and GLU320. The non-covalent bonding forces between receptors and ligands were hydrogen bonds, hydrophobic bonds, and electrostatic interactions (Xu et al., 2019b). The results showed that the interaction site of integrin  $\alpha 5\beta 1$  (PDB: 3VI4) with RGDN was similarly to the binding site of integrin  $\alpha 5\beta 1$  (PDB: 3VI4) with IERGDVVVQDSPSD, named GLU320, SER227, PHE187, and LEU225. The interacting amino acids of integrin  $\alpha\text{v}\beta 3$  (PDB: 1L5G) with c(RGDf-MVA) were LYS253, ALA218, ASR217, ALA215, GLU220, TYR122, ASN215, SER121, and TYR178. The interaction sites of IERGDVVVQDSPSD with integrin  $\alpha\text{v}\beta 3$  (PDB: 1L5G) were LYS119, GLU121,

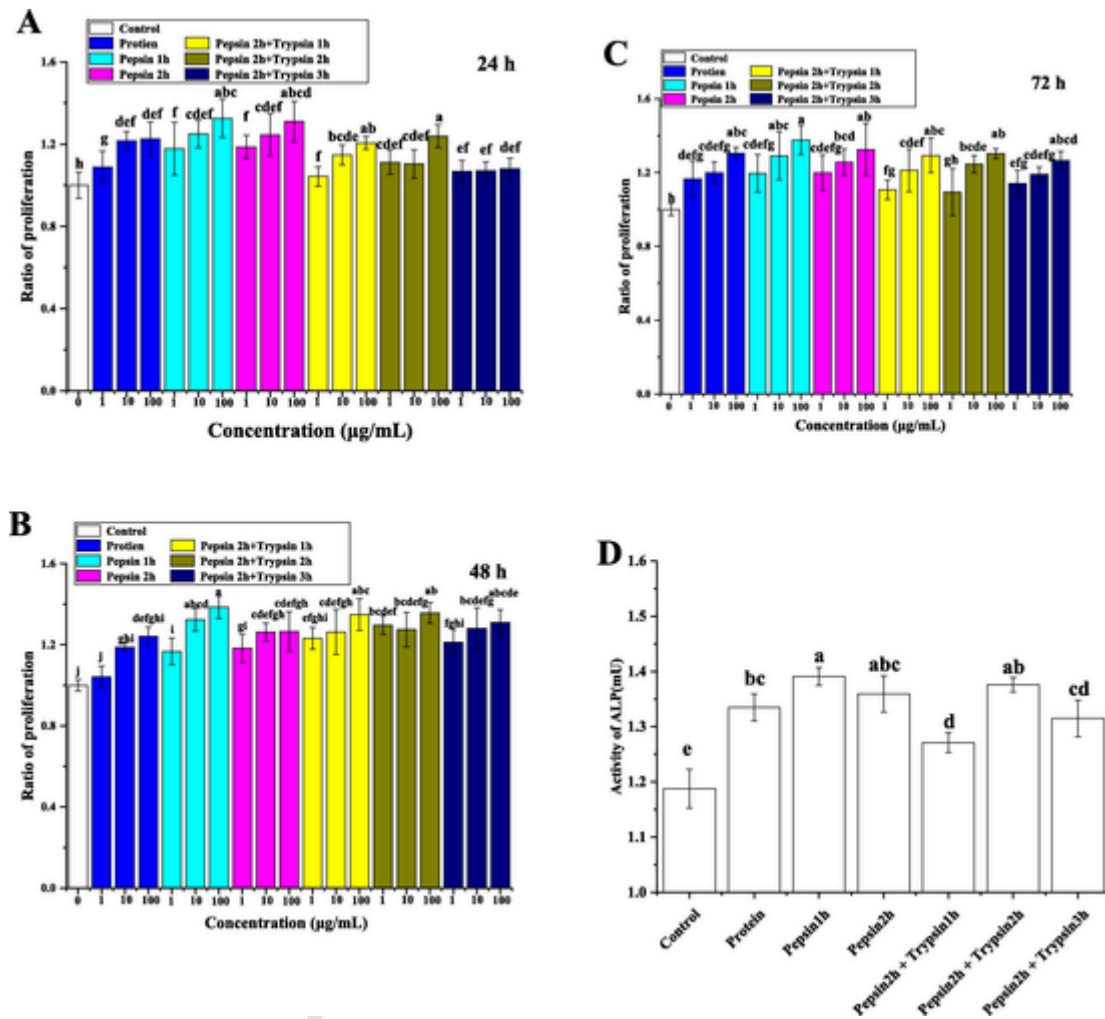


**Fig. 2.** Effects of WPL and hydrolysates on osteoblast proliferation and ALP activity. (A) The MC3T3-E1 treated by WPL and hydrolysates in 1, 10, 100 µg/mL for 24 h, 48 h, 72 h. (B) Effects of WPL and hydrolysates in 1, 10, 100 µg/mL on activity of ALP at 24 h, 48 h, 72 h. All statistical tests were conducted and values designated by different letters are statistically different ( $p < 0.05$ ).

**Table 2**  
Peptides identified by UPLC- Q Exactive™ HF-X and molecular docking analysis of the peptides by Discovery Studio.

No.	m/z	z	AA sequence	-CDOCKER energy for 3V14	-CDOCKER energy for 1L5G	Accession	Protein	PI	Net charge	Hydro	Ratio of hydrophilic AA
			RGDN <sup>a</sup>	116.249							
			c(RGDf-MVA) <sup>b</sup>		85.2449						
1	758.3679	2	IERGDVVVQDSPSD	177.434	193.908	A0A6G0J614	Transmembrane protein 182 OS = <i>Larimichthys crocea</i> OX = 215358 GN = D5F01_LYC01543 PE = 3 SV = 1	3.5	-3.0	0.7	57 %
2	664.3644	2	RGDLGIEIPTEK	183.402	184.115	A0A6G0IXB2	Pyruvate kinase OS = <i>Larimichthys crocea</i> OX = 215358 GN = D5F01_LYC04913 PE = 3 SV = 1	4.5	-1.0	0.8	42 %

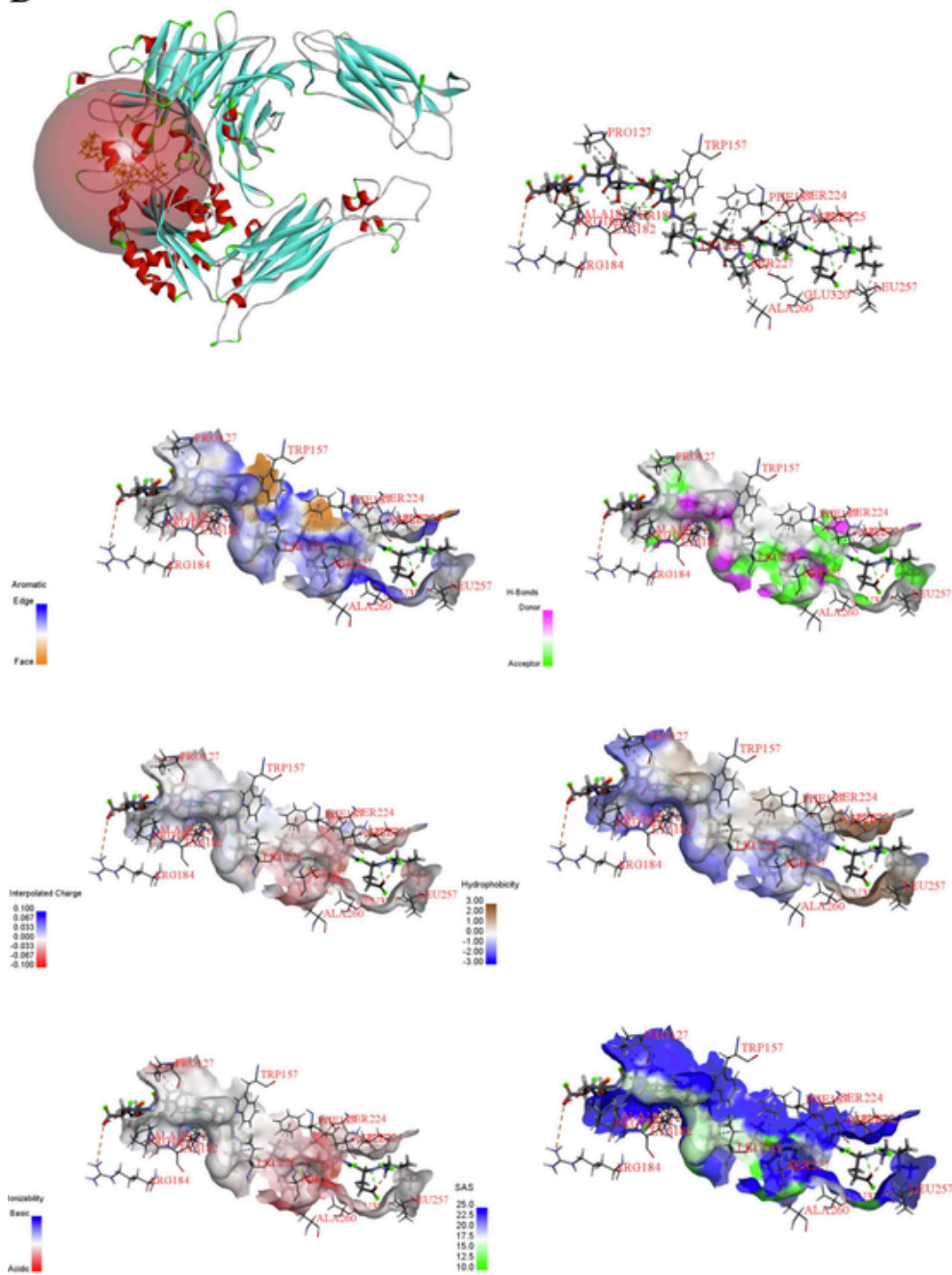
ASP126, ASP148, ALA149, ASP150, TYR166, TYR178, ARG214, ASN215, ARG216, ALA218, ASP251, and ASN313, respectively. The forces between receptors and ligands were aromatic, H-bonds, hydrophobicity and ionizability interactions. The abovementioned results showed that the interaction site of integrin  $\alpha 5\beta 1$  (PDB: 3V14) with RGDN was similarly to the binding site of integrin  $\alpha 5\beta 1$  (PDB: 3V14) with IERGDVVVQDSPSD, named GLU320, SER227, PHE187, and LEU225. The binding site between IERGDVVVQDSPSD and integrin  $\alpha \nu \beta 3$  (PDB: 1L5G) was similarly to that of c(RGDf-MVA) interacting with integrin  $\alpha \nu \beta 3$  (PDB: 1L5G), such as TYR178, ASN215, and

ALA218. Therefore, IERGDVVVQDSPSD had good binding ability to integrins (PDB: 1L5G, 3V14).

The interaction between RGDGIEIPTEK and integrin (PDB: 1L5G, 3V14) is shown in Fig. 3. The amino acids that RGDN interacted with integrin  $\alpha 5\beta 1$  (PDB: 3V14) were SER132, SER134, LYS182, PHE187, CYS187, ASN224, LEU225, ASP226, SER227, GLU229, ASP259, and GLU320. With regard to RGDGIEIPTEK interacted with integrin  $\alpha 5\beta 1$  (PDB: 3V14), the related amino acids were LYS182, ILE225, TYR226, ASP227, ASP228, SER229, LYS254, GLY255, ASN256, LEU257, and GLU320. The non-covalent interactions between receptors and ligands were hydrogen bonds, hydrophobic bonds, and electrostatic interac-



**B**



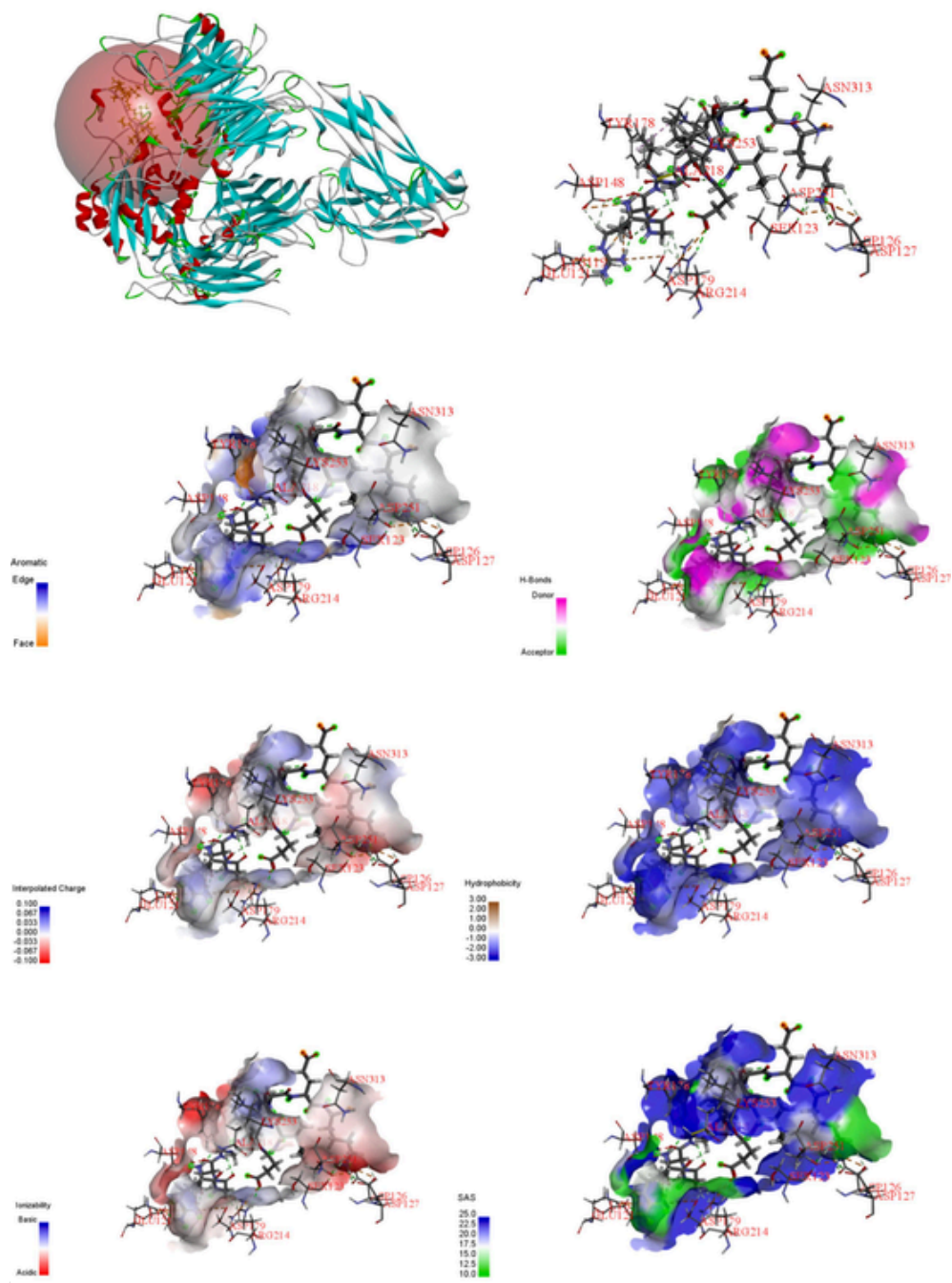
**3VI4**

(caption on next page)





C



1L5G

(caption on next page)

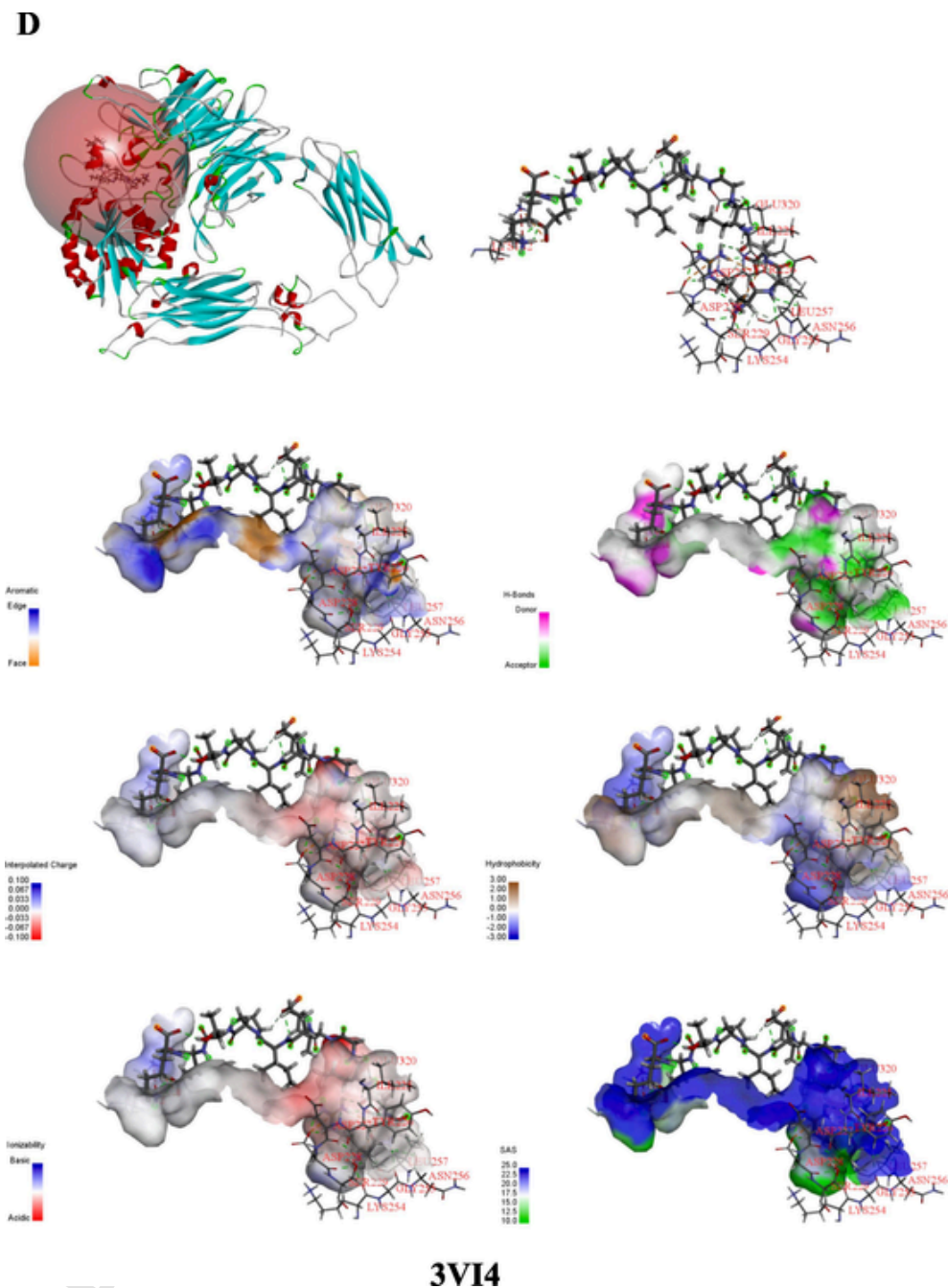


**Fig. 3.** Docking calculations for the interaction of IERGDVVVQDPSPD and RGDLGIEIPTEK with integrins: (A) Interaction sites of peptide IERGDVVVQDPSPD and amino acids on the integrin (PDB:1L5G). (B) Interaction sites of peptide IERGDVVVQDPSPD and amino acids on the integrin (PDB:3VI4). (C) Interaction sites of peptide RGDLGIEIPTEK and amino acids on the integrin (PDB:1L5G). (D) Interaction sites of peptide RGDLGIEIPTEK and amino acids on the integrin (PDB:3VI4). (B-D) The forces between receptors and ligands are aromatic, H-bonds, interpolated charge, hydrophobicity, ionizability and SAS interactions.

tions. As shown in Fig. 3, integrin  $\alpha\beta3$  (PDB: 1L5G) interacted with c(RGDF-MVA) by LYS253, GLU220, ASR217, TYR122, SER121, ALA215, ALA218, TYR178, and ASN215, respectively. The interaction sites of RGDGIEIPTEK with integrin  $\alpha\beta3$  (PDB: 1L5G) were LYS119, GLU121, SER123, ASP126, ASP127, ASP148, TYR178, ASP179, ARG214, ALA218, ASP251, LYS253, and ASN313, respectively (Fig. 3). The interactions between receptors and ligands were aromatic, H-bonds, hydrophobicity, and ionizability interactions. The binding site of RGDGIEIPTEK to integrin  $\alpha\beta3$  (PDB: 1L5G) was similarly to that of c(RGDF-MVA) interacting with integrin  $\alpha\beta3$  (PDB: 1L5G), such as TYR178, ALA218, and LYS253. Therefore, RGDGIEIPTEK could be well combined with integrin (PDB: 1L5G, 3VI4) and revealed good binding ability. The results showed that IERGDVVVQDPSPD and RGDGIEIPTEK

could promote the proliferation of pre-osteoblasts and inhibit the proliferation of osteoclasts.

### 3.7. Osteogenic activity of the identified peptides

The HPLC results of peptides are shown in Figure S1 (Supplementary information). The purities of the peptides IERGDVVVQDPSPD and RGDGIEIPTEK were 95.39 % and 94.36 %, respectively, and the retention time were 11.147 and 10.966 min, respectively. The peptide sequences and mass spectra obtained by HPLC coupled with mass spectrometry ( $m/z$ ) of IERGDVVVQDPSPD and RGDGIEIPTEK were 1516.89 and 1327.51, respectively.

Osteoblast proliferation and ALP activity can be used to verify osteogenic activity. MC3T3-E1 pre-osteoblasts were cultured at 100 µg/mL of peptide for 72 h. As shown in Fig. 4, compared with the control cells, pre-osteoblasts increased by 32.16 % and 26.23 % after 72 h treatment with 100 µg/mL polypeptides IERGDVVVQDSPSD and RGDDLGIPIPEK, respectively. At the same time, the ALP activity after the treatment of IERGDVVVQDSPSD and RGDDLGIPIPEK peptides (100 µg/mL) were  $1.87 \pm 0.04$  and  $1.77 \pm 0.04$  mU, respectively, which had the increase of 45.18 % and 36.67 % than the control group (Fig. 4) ( $p < 0.05$ ). The osteogenic activity of these two peptides was better than that of the peptide YRGDVPK, the increasing rate in the peptide YRGDVPK of 100 nM was 23.68 % (Chen et al., 2019).

#### 4. Conclusions

Our results showed that the extracted large yellow croaker protein WPL had remarkable *in vitro* osteogenic activity. Particularly, the protein hydrolyzates of P1 and P2 groups revealed higher activity, inducing the viability increase of  $37.60 \pm 7.97$  % and  $32.47 \pm 14.15$  % in MC3T3-E1 osteoclasts. In addition, the alkaline phosphatase activity levels were  $1.39 \pm 0.02$  mU and  $1.36 \pm 0.03$  mU, respectively. By analyzing the molecular weight distribution and free amino acid composition of each hydrolysis stage, the available nutrients in the proteins were also determined. Peptide IERGDVVVQDSPSD in group P1 and peptide RGDLGIPIPEK in group P2 could promote the proliferation of osteoblasts as well as enhance the ALP activity. The -CDOCKER ener-

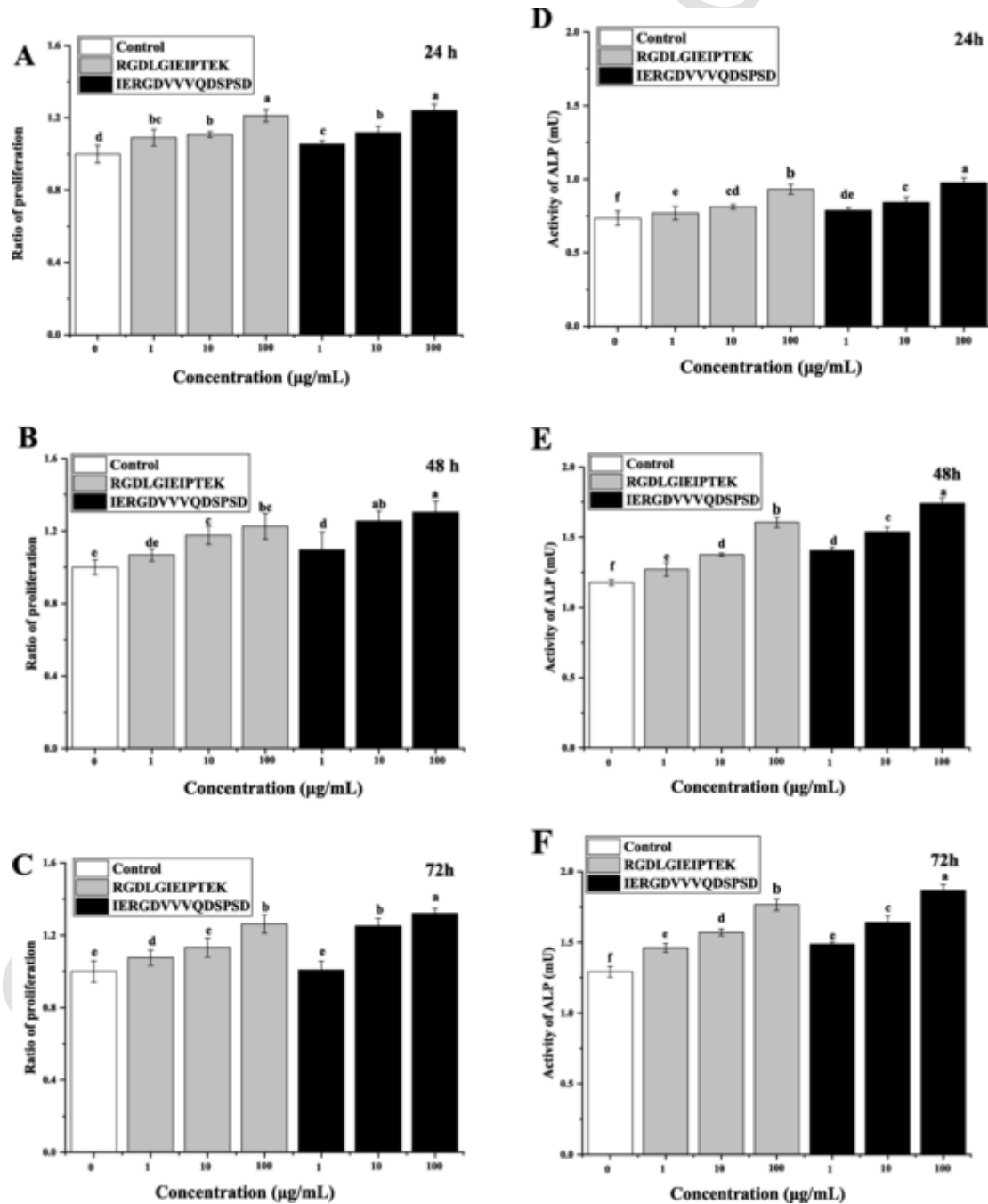


Fig. 4. Osteogenic activity of the peptide IERGDVVVQDSPSD and RGDLGIPIPEK. (A-C) The MC3T3-E1 treated by peptide IERGDVVVQDSPSD and RGDLGIPIPEK in 1, 10, 100 µg/mL for 24 h, 48 h, 72 h. (D-F) Effects of 100 µg/mL peptide IERGDVVVQDSPSD and RGDLGIPIPEK on ALP activity at 24, 48, and 72 h. All statistical tests (n = 6) were conducted, and values designated by different letters are considered significantly different ( $p < 0.05$ ).

gies of the peptides IERGDVVVQDPSD and RGDDLGLIEIPTEK with one integrin (PDB: 3VI4) were 177.434 and 183.402 kcal/mol, respectively, while the -CDOCKER energies with another integrin (PDB: 1L5G) were 193.908 and 184.115 kcal/mol, respectively. Hence, the peptides had stronger interaction with RGD than integrins (PDB: 3VI4 and 1L5G). To conclude, WPL can be used as an effective ingredient for promoting bone growth.

Canalis, Economides, & Gaggero, 2003; Hyung, Ahn, & Je, 2018; Je, Park, Hwang, & Ahn, 2015; Jeong et al., 2018; Kim, Kim, Jung, Hong, & Lee, 2014; Laemmli, 1970; Lemieux, Horowitz, & Kacena, 2010; G. Li, Ryaby, Carney, & Wang, 2005; W. Li, Zhu, & Hu, 2015; Lin, Zhang, Han, & Cheng, 2017; Min, Kang, Jung, Jang, & Min, 2018; Nagel et al., 2004; Rao, Head, Kulkarni, & LaLonde, 2007; Takagi, Strokovich, Springer, & Walz, 2003; Tsai, Chen, Wei, Tan, & Lai, 2010; Wu, Robertson, Brooks, & Vieth, 2003; Xu et al., 2019a–c; Yang et al., 2021

#### CRedit authorship contribution statement

**Zhe Xu** : Validation, Formal analysis, Investigation, Writing – original draft, Data curation, Writing – original draft. **Shiying Han** : Data curation, Writing – review & editing. **Hui Chen** : Methodology, Supervision. **Lingyu Han** : Writing – review & editing. **Xiufang Dong** : Writing – review & editing. **Maolin Tu** : Writing – review & editing. **Zhijian Tan** : Conceptualization, Methodology, Supervision, Writing – review & editing. **Ming Du** : Conceptualization, Methodology, Supervision, Resources, Writing – review & editing. **Tingting Li** : Resources, Writing – review & editing, Project administration, Funding acquisition.

#### Declaration of Competing Interest

The authors declare that they have no known competing financial interests or personal relationships that could have appeared to influence the work reported in this paper.

#### Acknowledgements

This work was supported by the National Key R&D Program of China (2018YFD0400601), the Zhejiang provincial key laboratory of efficient development and utilization of deep blue fishery resources projects supported by the open fund (SL2021004).

#### Appendix A. Supplementary data

Supplementary data to this article can be found online at <https://doi.org/10.1016/j.foodres.2022.112238>.

#### References

- Ashe, H. L. (2016). *Modulation of BMP signalling by integrins*. *Biochemical Society Transactions*, 44(5), 1465–1473.
- Chen H. Xu Z. Fan F. Shi P. Tu M. Wang Z. Du M. 2019 Identification and mechanism evaluation of a novel osteogenesis promoting peptide from tubulin alpha-1C chain in *Crassostrea gigas* Food Chemistry 272 751 757
- Cornish J. Callon K. E. Naot D. Palmano K. P. Banovic T. Bava U. ... Chen Q. 2004 Lactoferrin is a potent regulator of bone cell activity and increases bone formation *in vivo* Endocrinology, 145(9) 4366 4374
- Fan, F., Tu, M., Liu, M., Shi, P., Wang, Y., & Wu, D. (2017). *Isolation and characterization of lactoferrin peptides with stimulatory effect on osteoblast proliferation*. *Journal of Agricultural and Food Chemistry*, 65(33), 7179–7185.
- Bharadwaj, S., Naidu, A., Betageri, G., Prasadarao, N., & Naidu, A. (2009). *Milk ribonuclease-enriched lactoferrin induces positive effects on bone turnover markers in postmenopausal women*. *Osteoporosis International*, 20(9), 1603–1611.

- Blais, A., Malet, A., Mikogami, T., Martin-Rouas, C., & Tomé, D. (2009). *Oral bovine lactoferrin improves bone status of ovariectomized mice*. *American Journal of Physiology*, 296(6), E1281–E1288.
- Canalis, E., Economides, A. N., & Gaggero, E. (2003). *Bone morphogenetic proteins, their antagonists, and the skeleton*. *Endocrine Reviews*, 24(2), 218–235.
- Chen, C., Cheng, P., Xie, H., Zhou, H. D., Wu, X. P., & Liao, E. Y. (2014). *MiR-503 regulates osteoclastogenesis via targeting RANK*. *Journal of Bone & Mineral Research the Official Journal of the American Society for Bone & Mineral Research*, 29(2), 338–347.
- Danen, E. H., & Yamada, K. M. (2001). *Fibronectin, integrins, and growth control*. *Journal of Cellular Physiology*, 189(1), 1–13.
- Fernández-Musoles, R., Manzanares, P., Burguete, M.C., Alborch, E., & Salom, J.B. (2013). *In Vivo angiotensin I-converting enzyme inhibition by long-term intake of antihypertensive lactoferrin hydrolysate in spontaneously hypertensive rats*. *Food Research International*, 54(1), 627–632.
- Georgy, S.R., Pagel, C., Ghasem-Zadeh, A., Zebaze, R., Pike, R., Sims, N., & Mackie, E. (2012). *Proteinase-activated receptor-2 is required for normal osteoblast and osteoclast differentiation during skeletal growth and repair*. *Bone*, 50(3), 704–712.
- Ghassem, M., Fern, S. S., Said, M., Ali, Z. M., Ibrahim, S., & Babji, A. S. (2014). *Kinetic characterization of Channa striatus muscle sarcoplasmic and myofibrillar protein hydrolysates*. *Journal of Food Science & Technology*, 51(3), 467–475.
- Haider M.-T. Hunter K. D. Robinson S. P. Graham T. J. Corey E. Dear T. N. ... Holen I. 2015 Rapid modification of the bone microenvironment following short-term treatment with Cabozantinib *in vivo* Bone 81 581 592
- Jeong, Y., Jo, Y. K., Kim, B. J., Yang, B., Joo, K. I., & Cha, H. J. (2018). *Sprayable adhesive nanotherapeutics: mussel-protein-based nanoparticles for highly efficient locoregional cancer therapy*. *ACS Nano*, 12(9), 8909–8919.
- Kang, E.-S., Kim, D.-S., Han, Y., Son, H., Chung, Y.-H., Min, J., & Kim, T.-H. (2018). *Three-dimensional graphene-RGD peptide nanosand composites that enhance the osteogenesis of human adipose-derived mesenchymal stem cells*. *International Journal of Molecular Sciences*, 19(3), 669.
- Hughes, F.J., Turner, W., Belibasakis, G., & Martuscelli, G. (2006). *Effects of growth factors and cytokines on osteoblast differentiation*. *Periodontol*, 41(1), 48–72.
- Hyung, J.-H., Ahn, C.-B., & Je, J.-Y. (2018). *Blue mussel (Mytilus edulis) protein hydrolysate promotes mouse mesenchymal stem cell differentiation into osteoblasts through up-regulation of bone morphogenetic protein*. *Food Chemistry*, 242, 156–161.
- Je J.-Y. Park S. Y. Hwang J.-Y. Ahn C.-B. 2015 Amino acid composition and *in vitro* antioxidant and cytoprotective activity of abalone viscera hydrolysate *Journal of Functional Foods* 16 94 103
- Kim, E.-C., Kim, T.-H., Jung, J.-H., Hong, S. O., & Lee, D.-W. (2014). *Enhanced osteogenic differentiation of MC3T3-E1 on rhBMP-2-immobilized titanium via click reaction*. *Carbohydrate, Polymers*, 103, 170–178.
- Liu, H., Tu, M., Cheng, S., Xu, Z., Xu, X., & Du, M. (2019). *Anticoagulant decapeptide interacts with thrombin at the active site and exosite-I*. *Journal of Agricultural and Food Chemistry*, 68(1), 176–184.
- Lorget F. Clough J. Oliveira M. Daury M.-C. Sabokbar A. Offord E. 2002 Lactoferrin reduces *in vitro* osteoclast differentiation and resorbing activity *Biochemical and Biophysical Research Communications* 296 2 261 266
- Kim, K., Kim, J.H., Kim, I., Seong, S., & Kim, N. (2018). *TRIM38 regulates NF-κB activation through TAB2 degradation in osteoclast and osteoblast differentiation*. *Bone*, 113, 17–28.
- Laemmli, U. K. (1970). *Cleavage of structural proteins during the assembly of the head of bacteriophage T4*. *Nature*, 227(5259), 680–685.
- Lemieux, J. M., Horowitz, M. C., & Kacena, M. A. (2010). *Involvement of integrins α3β1 and α5β1 and glycoprotein IIb in megakaryocyte-induced osteoblast proliferation*. *Journal of Cellular Biochemistry*, 109(5), 927–932.
- Li, G., Ryaby, J. T., Carney, D. H., & Wang, H. (2005). *Bone formation is enhanced by thrombin-related peptide TP508 during distraction osteogenesis*. *Journal of Orthopaedic Research*, 23(1), 196–202.
- Li, W., Zhu, S., & Hu, J. (2015). *Bone regeneration is promoted by orally administered bovine lactoferrin in a rabbit tibial distraction osteogenesis model*. *Clinical Orthopaedics & Related Research*, 473(7), 2383–2393.
- Lin, K., Zhang, L.-w., Han, X., & Cheng, D.-y. (2017). *Novel*

- angiotensin I-converting enzyme inhibitory peptides from protease hydrolysates of Qula casein: Quantitative structure-activity relationship modeling and molecular docking study. *Journal of Functional Foods*, 32, 266–277.
- Mada, S.B., Reddi, S., Kumar, N., Kumar, R., Kapila, S., Kapila, R., ... Ahmad, N. (2017). Antioxidative peptide from milk exhibits antiosteopenic effects through inhibition of oxidative damage and bone-resorbing cytokines in ovariectomized rats. *Nutrition*, 43, 21–31.
- Mai, Z., Peng, Z., Wu, S., Zhang, J., Chen, L., Liang, H., ... Ai, H. (2013). Single bout short duration fluid shear stress induces osteogenic differentiation of MC3T3-E1 cells via integrin  $\beta 1$  and BMP2 signaling cross-talk. *Plos One*, 8(4), e61600.
- Nagel, D., Khosla, S., Sanyal, A., Rosen, D., Kumagai, Y., & Riggs, B. L. (2004). A fragment of the hypophosphatemic factor, MEPE, requires inducible cyclooxygenase-2 to exert potent anabolic effects on normal human marrow osteoblast precursors. *Journal of Cellular Biochemistry*, 93(6), 1107–1114.
- Naot, D., Chhana, A., Matthews, B. G., Callon, K. E., Tong, P. C., Lin, J.-M., ... Cornish, J. (2011). Molecular mechanisms involved in the mitogenic effect of lactoferrin in osteoblasts. *Bone*, 49(2), 217–224.
- Min, S.-K., Kang, H. K., Jung, S. Y., Jang, D. H., & Min, B.-M. (2018). A vitronectin-derived peptide reverses ovariectomy-induced bone loss via regulation of osteoblast and osteoclast differentiation. *Cell Death & Differentiation*, 25(2), 268–281.
- Oh, S.-H., Kim, J.-W., Kim, Y., Lee, M.N., Kook, M.-S., Choi, E.Y., ... Koh, J.-T. (2017). The extracellular matrix protein Edil3 stimulates osteoblast differentiation through the integrin  $\alpha 5 \beta 1$ /ERK/Runx2 pathway. *Plos One*, 12(11), e0188749.
- Pandey, M., Kapila, S., Kapila, R., Trivedi, R., & Karvande, A. (2018). Evaluation of the osteoprotective potential of whey derived-antioxidative (YVEEL) and angiotensin-converting enzyme inhibitory (YLLF) bioactive peptides in ovariectomized rats. *Food & Function*, 9(9), 4791–4801.
- Park, D., Park, C.-W., Choi, Y., Lin, J., Seo, D.-H., Kim, H.-S., ... Kang, I.-C. (2016). A novel small-molecule PPI inhibitor targeting integrin  $\alpha v \beta 3$ -osteopontin interface blocks bone resorption in vitro and prevents bone loss in mice. *Biomaterials*, 98, 131–142.
- Rao, S. N., Head, M. S., Kulkarni, A., & LaLonde, J. M. (2007). Validation studies of the site-directed docking program LibDock. *Journal of Chemical Information & Modeling*, 47(6), 2159–2171.
- Ruiz-Giménez, P., Salom, J.B., Marcos, J.F., Vallés, S., Martínez-Maqueda, D., Recio, I., ... Manzanares, P. (2012). Antihypertensive effect of a bovine lactoferrin pepsin hydrolysate: identification of novel active peptides. *Food Chemistry*, 131(1), 266–273.
- Shi, P., Liu, M., Fan, F., Chen, H., Yu, C., Lu, W., & Du, M. (2018). Identification and mechanism of peptides with activity promoting osteoblast proliferation from bovine lactoferrin. *Food Bioscience*, 22, 19–25.
- Song, S., Zhang, B., Wu, S., Huang, L., Ai, C., Pan, J., ... Wen, C. (2018). Structural characterization and osteogenic bioactivity of a sulfated polysaccharide from pacific abalone (*Haliotis discus hannai* Ino). *Carbohydrate Polymers*, 182, 207–214.
- Tak, Y., Kaur, M., Amarowicz, R., Bhatia, S., & Gautam, C. (2021). Pulse derived bioactive peptides as novel nutraceuticals: A review. *International Journal of Peptide Research and Therapeutics*, 27(3), 2057–2068.
- Takagi, J., Strokovich, K., Springer, T. A., & Walz, T. (2003). Structure of integrin  $\alpha 5 \beta 1$  in complex with fibronectin. *EMBO Journal*, 22(18), 4607–4615.
- Tang, S.-Y., Xie, H., Yuan, L.-Q., Luo, X.-H., Huang, J., Cui, R.-R., ... Liao, E.-Y. (2007). Apelin stimulates proliferation and suppresses apoptosis of mouse osteoblastic cell line MC3T3-E1 via JNK and PI3-K/Akt signaling pathways. *Peptides*, 28(3), 708–718.
- Wang X. Guo H. Zhang W. Wen P. Zhang H. Guo Z. Ren F. (2013) Effect of iron saturation level of lactoferrin on osteogenic activity in vitro and in vivo *Journal of Dairy Science* 96 1 33 39
- Tsai, W.-B., Chen, R. P.-Y., Wei, K.-L., Tan, S.-F., & Lai, J.-Y. (2010). Modulation of RGD-functionalized polyelectrolyte multilayer membranes for promoting osteoblast function. *Journal of Biomaterials Science, Polymer, Edition*, 21(3), 377–394.
- Wu, G., Robertson, D. H., Brooks, & Vieth, M. (2003). Detailed analysis of grid-based molecular docking: A case study of CDOCKER—A CHARMM-based MD docking algorithm. *Journal of Computational Chemistry*, 24(13), 1549–1562.
- Xiong, J.-P., Stehle, T., Zhang, R., Joachimiak, A., Frech, M., Goodman, S.L., & Arnaout, M.A. (2002). Crystal structure of the extracellular segment of integrin  $\alpha v \beta 3$  in complex with an Arg-Gly-Asp ligand. *Science*, 296(5565), 151–155.
- Xu, Z., Chen, H., Fan, F., Shi, P., Cheng, S., & Tu, M. (2020). Pharmacokinetics and transport of an osteogenic dodecapeptide. *Journal of Agricultural and Food Chemistry*, 68(37), 9961–9967.
- Xu, Z., Chen, H., Fan, F., Shi, P., Tu, M., & Cheng, S. (2019a). Bone formation activity of an osteogenic dodecapeptide from blue mussels (*Mytilus edulis*). *Food & Function*, 10(9), 5616–5625.
- Xu, Z., Chen, H., Wang, Z., Fan, F., Shi, P., & Tu, M. (2019b). Isolation and characterization of peptides from *mytilus edulis* with osteogenic activity in mouse MC3T3-E1 preosteoblast cells. *Journal of Agricultural and Food Chemistry*, 67(5), 1572–1584.
- Xu, Z., Zhao, F., Chen, H., Xu, S., Fan, F., & Shi, P. (2019c). Nutritional properties and osteogenic activity of enzymatic hydrolysates of proteins from the blue mussel (*Mytilus edulis*). *Food & Function*, 10(12), 7745–7754.
- Yang, F., Williams, C.G., Wang, D.-A., Lee, H., Manson, P.N., & Elisseeff, J. (2005). The effect of incorporating RGD adhesive peptide in polyethylene glycol diacrylate hydrogel on osteogenesis of bone marrow stromal cells. *Biomaterials*, 26(30), 5991–5998.
- Yang, M., Xu, Z., Wu, D., Dong, Y.u., Wang, Z., & Du, M. (2021). Characterizations and the mechanism underlying osteogenic activity of peptides from enzymatic hydrolysates of *Stichopus japonicus*. *Journal of Agricultural and Food Chemistry*, 69(51), 15611–15623.
- Zhang, J.-Q., Luo, Y.-J., Xiong, Y.-S., Yu, Y., Tu, Z.-C., Long, Z.-J., ... Weng, J. (2016). Design, synthesis, and biological evaluation of substituted pyrimidines as potential phosphatidylinositol 3-kinase (PI3K) inhibitors. *Journal of Medicinal Chemistry*, 59(15), 7268–7274.
- Zhou, S., Zu, Y., Zhuang, F., & Yang, C. (2015). Hypergravity-induced enrichment of  $\beta 1$  integrin on the cell membranes of osteoblast-like cells via caveolae-dependent endocytosis. *Biochemical & Biophysical Research Communications*, 463(4), 928–933.